

## Microwave Lens for Polar Molecules

Hitoshi Odashima,<sup>1,2</sup> Simon Merz,<sup>1</sup> Katsunari Enomoto,<sup>1,3</sup> Melanie Schnell,<sup>1,\*</sup> and Gerard Meijer<sup>1</sup>

<sup>1</sup>*Fritz-Haber-Institut der Max-Planck-Gesellschaft, Faradayweg 4-6, D-14195 Berlin, Germany*

<sup>2</sup>*Department of Physics, Meiji University, Kawasaki 214-8571, Japan*

<sup>3</sup>*Department of Physics, University of Toyama, Toyama 930-8555, Japan*

(Received 31 March 2010; published 23 June 2010)

We here report on the implementation of a microwave lens for neutral polar molecules suitable to focus molecules in both low-field-seeking and high-field-seeking states. By using the  $TE_{11m}$  modes of a 12 cm long cylindrically symmetric microwave resonator, Stark-decelerated ammonia molecules are transversally confined. We investigate the focusing properties of this microwave lens as a function of the molecules' velocity, the microwave power, and the frequency detuning  $\Delta$  from the molecular resonance. Such a microwave lens can be seen as a first important step towards further microwave devices, such as decelerators and traps.

DOI: 10.1103/PhysRevLett.104.253001

PACS numbers: 37.20.+j, 33.20.Bx, 37.10.Mn

Since the early 1920s, external electric and magnetic fields have been used in ever more sophisticated setups to gain increasing control over the molecules' degrees of freedom. As a first step, both an electric and a magnetic deflector have been realized [1,2], which allowed the selection of single quantum states to perform groundbreaking new experiments. In the mid 1950s, the implementation of an electrostatic quadrupole lens allowed Townes and co-workers to demonstrate the MASER by exploiting the different focusing properties of the  $|J, K\rangle = |1, 1\rangle$  inversion doublet levels of the vibronic ground state of ammonia [3]. By now, it has become possible to decelerate and trap neutral molecules in the gas phase using switched electric or magnetic fields, enabling novel experiments in the field of cold molecules [4–6].

Besides external electric and magnetic fields, also electromagnetic radiation can be used to manipulate the motion of molecules. For example, an optical decelerator has been implemented [7,8]. Optical dipole traps are widespread in the field of cold atoms [9]. In 1975, Hill and Gallagher implemented a deflector based on a rectangular microwave resonator [10], the simplest molecule-manipulation device using microwave radiation. They detected the deflection of a beam of CsF molecules, but their experimental results could not be fully understood and they did not pursue these experiments.

In this Letter, we demonstrate and characterize a microwave lens for polar molecules, which allows us to focus polar molecules using microwave radiation. A packet of supersonically expanded ammonia molecules ( $^{14}\text{NH}_3$ ) is decelerated to low velocities of around 20 m/s using a Stark decelerator. Subsequently, they enter a cylindrically symmetric microwave resonator. The applied microwave field prevents the molecules from spreading out in transverse directions; i.e., it acts like a positive lens on polar molecules. For this, we exploit the same inversion transition as Townes and co-workers used in their original MASER experiments.

The force exerted on a molecule in microwave fields depends on its dipole moment, the sign and the magnitude of the detuning of the microwave frequency from the molecular resonance frequency, and the microwave field strength. High input powers and high- $Q$  cavities are available, so that, in principle, large field strengths can be achieved. Furthermore, in contrast to optical fields, very small detunings can be exploited due to the long lifetime of the states coupled in the microwave transition. Such small detunings in turn lead to strong interaction forces. In addition, for microwave manipulation the direction of the interaction force (ac Stark effect [11]) depends on the sign of the detuning. Thus, both molecules in low-field-seeking and in high-field-seeking states can be affected. This is particularly advantageous for large molecules and molecules in their internal ground state, which are always high-field seeking in dc electric fields. To focus, decelerate, and trap them using electric fields, dynamic focusing has to be applied [12,13], which leads to stringent experimental demands. Here, microwave fields could be a promising alternative. The lens demonstrated in this work can be seen as an important step towards the realization of microwave deceleration and trapping devices, which have been suggested recently [14,15].

The interaction energy of polar molecules with microwave radiation is based on the ac Stark effect. For ammonia, the energy of the inversion doublet levels as a function of the microwave field strength (Fig. 1) can be written to a good approximation as

$$E_{AC}(\rho, \varphi, z) = \frac{h\Delta}{2} \pm \sqrt{\left(\frac{h\Delta}{2}\right)^2 + \left(\frac{E_0(\rho, \varphi, z)\mu MK}{2J(J+1)}\right)^2}, \quad (1)$$

with the molecular dipole moment  $\mu$ , the total angular momentum quantum number  $J$ , and the projections of the total angular momentum onto the molecular symmetry axis  $K$  and the electric field axis  $M$ , respectively.  $\Delta = \nu - \nu_0$  is the so-called detuning defined as the difference of the applied microwave frequency  $\nu$  from the molecular reso-

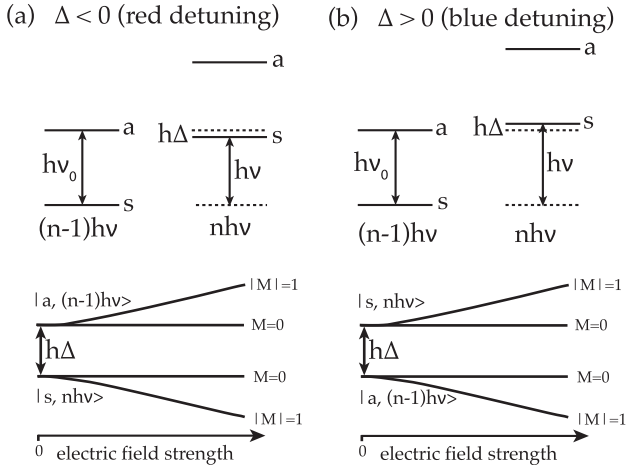


FIG. 1. Dressed-state picture and ac Stark shift of the  $|J, K\rangle = |1, 1\rangle$  inversion doublet of  $^{14}\text{NH}_3$  for (a) red ( $\Delta < 0$ ) and (b) blue ( $\Delta > 0$ ) detuning. Depending on the detuning, either the symmetric ( $s$ ) lower level ( $\Delta < 0$ ) or the antisymmetric ( $a$ ) upper level ( $\Delta > 0$ ) of the inversion doublet becomes high-field seeking in microwave fields.

nance frequency  $\nu_0 \approx 23\,695$  MHz (inversion transition of the  $|J, K\rangle = |1, 1\rangle$  level of the vibronic ground state of  $^{14}\text{NH}_3$ ) and  $h$  is Planck's constant.  $E_0(\rho, \varphi, z)$  is the electric field strength of the microwave field, as defined below. Its maximum value  $\epsilon_{\text{MW}}$  is given by  $\epsilon_{\text{MW}} \approx \sqrt{Q_0 U_0^2 P / (\pi \nu \epsilon_0)}$  [16]. Here,  $Q_0$  is the quality factor of the resonator and  $U_0^2$  is a geometrical factor which can be approximated by  $4.2/V$  for  $\text{TE}_{11m}$  modes (*vide infra*) in a cylindrically symmetric resonator, with  $V$  being the resonator volume.  $P$  is the microwave power coupled into the resonator and  $\epsilon_0$  the permittivity of free space. Consequently, the focusing force in a microwave lens depends on the molecular dipole moment  $\mu$ , the resonator, the microwave power  $P$ , and the sign and the magnitude of the detuning  $\Delta$ .

While the magnitude of  $\Delta$  determines the strength, its sign defines the direction of the focusing force; i.e., it determines whether a particular molecular state is attracted by a field maximum or a field minimum [Eq. (1)]. This is schematically displayed in Fig. 1 for the antisymmetric ( $a$ ) upper (low-field seeking in dc electric fields) and the symmetric ( $s$ ) lower energy levels (high-field seeking in dc electric fields) of the  $|J, K\rangle = |1, 1\rangle$  inversion doublet of  $^{14}\text{NH}_3$  molecules (see, for example, Ref. [17]). In the dressed-state picture, the molecular energy levels are “dressed” with the number of photons  $n$ . In this way, the  $s$  state dressed with  $n$  photons can come close to the  $a$  state with  $(n - 1)$  photons, resulting in a strong interaction. For small detunings, this leads to a linearization of the ac Stark energy. While for red detuning ( $\Delta < 0$ ) the  $a$  state is low-field seeking, it becomes high-field seeking for blue detuning ( $\Delta > 0$ ). This can be exploited for various applications, such as the manipulation of larger and more complex molecules. Here, we Stark decelerate  $^{14}\text{NH}_3$  molecules in

the  $a$  state, which is low-field seeking in dc electric fields. Subsequently, we can conveniently focus these molecules using blue detuned microwave radiation without having to transfer the molecules to a different state. Although such transfer can be performed in principle, it is accompanied by significant losses, as the population is distributed over a large number of hyperfine levels [13].

The experimental setup is schematically shown in Fig. 2(a). A detailed description of the molecular beam machine and, in particular, of the deceleration of a beam of ammonia molecules is given elsewhere [17]. The 120 mm long microwave resonator is made of copper and its entrance is located about 2.5 mm behind the end of the decelerator. It has an inner radius of 3.705 mm. The resonator is closed by two end caps with 3 mm holes to allow the molecules to fly through. The microwave radiation is coupled into the resonator using a dipole antenna, which is oriented along the  $y$  direction. The electric field component of the microwave field propagates parallel to the antenna; i.e., the electric field is linearly polarized perpendicular to

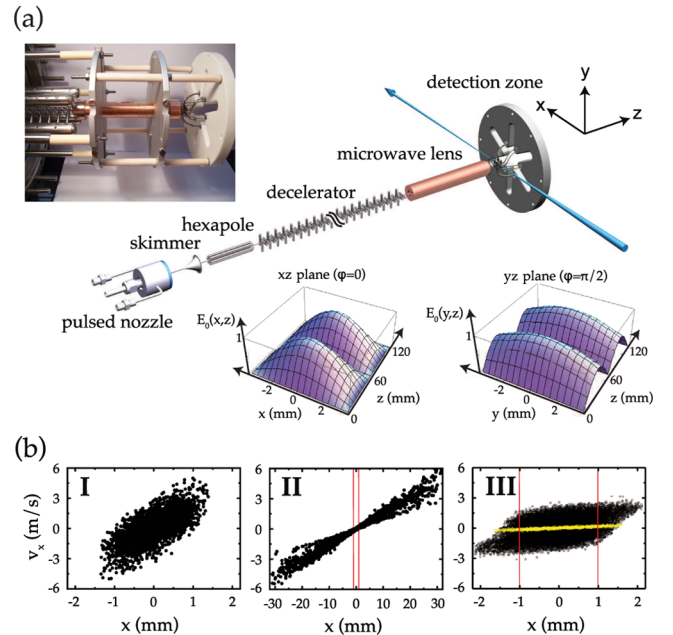


FIG. 2 (color online). (a) Scheme of the experimental setup, complemented by a photo showing the end of the decelerator, the microwave resonator, and the detection zone. The calculated electric field strength  $E_0(\rho, \varphi, z)$  for the  $\text{TE}_{112}$  mode is shown for two perpendicular planes of the resonator. Here,  $z$  is the symmetry axis of the resonator which coincides with the molecular beam axis. Note the different scales for the transverse and longitudinal directions. (b) Simulated transverse phase-space distributions of the molecules in the decelerated packet (i.e., their positions  $x$  and velocities  $v_x$ ): (I) at the beginning of the microwave resonator, (II) in the laser detection region if no microwave resonator would be integrated, and (III) at the same position but including the microwave resonator, with microwave radiation turned on (black circles,  $P = 3.5$  W) and turned off (narrow  $v_x$  distribution). In (II) and (III), the detection region along  $x$  is also indicated by vertical (red) lines.

the resonator axis (TE mode). In the experiment, we use  $TE_{11m}$  modes for focusing ammonia molecules. Here, 1, 1,  $m$  denote the number of maxima in radial ( $\rho$ ), azimuthal ( $\varphi$ ), and longitudinal ( $z$ ) direction, respectively. Since the antenna is located at half the length of the resonator,  $TE_{11m}$  modes with odd  $m$ , which have an electric field maximum at this position, are strongly perturbed. Here, we use the  $TE_{112}$  ( $\Delta = +71$  MHz) and the  $TE_{114}$  mode ( $\Delta = +459$  MHz) to confine the transverse motion of ammonia molecules. For these modes,  $Q_0$  is about 5000 [18].

The distribution of the electric field strength (mode pattern) for  $TE_{11m}$  modes in cylindrical coordinates can be calculated using

$$E_0(\rho, \varphi, z) = \epsilon_{\text{MW}} \frac{U(\rho, \varphi, z)}{U_0}, \quad (2)$$

with  $U(\rho, \varphi, z)$  giving the field distribution [19]:

$$U(\rho, \varphi, z) = 2U_0 \sqrt{\sin^2\left(\frac{m\pi z}{d}\right)} \times \sqrt{\left[\frac{J_1(\gamma\rho)}{\gamma\rho}\right]^2 \sin^2\varphi + \left[\frac{\partial J_1(\gamma\rho)}{\gamma\partial\rho}\right]^2 \cos^2\varphi}. \quad (3)$$

Here,  $J_1(\gamma\rho)$  is the Bessel function of first order.  $\gamma$  is defined as  $\gamma = x'_{11}/R$ , with  $x'_{11} = 1.841$  being the first root of the derivative of  $J_1(\gamma\rho)$  (for  $TE_{11m}$  modes).  $d$  and  $R$  are the length and the radius of the resonator, respectively.

In the inset of Fig. 2(a),  $E_0(\rho, \varphi, z)$  is shown for the  $TE_{112}$  mode for two perpendicular planes;  $E_0(x, z)$  for  $\varphi = 0$  and  $E_0(y, z)$  for  $\varphi = \pi/2$ . The electric field distribution exhibits a maximum on the resonator axis  $z$ , which decreases towards the resonator walls in transverse directions. Consequently, molecules in ac high-field-seeking states are transversally focused towards the resonator axis  $z$ . Note that the electric field distribution is not cylindrically symmetric, which leads to different gradients and thus different focusing strengths for the two transverse directions  $x$  and  $y$ .

In the experiment, decelerated packets of  $\text{NH}_3$  molecules leave the decelerator in the  $a$  state of the  $|J, K\rangle = |1, 1\rangle$  inversion doublet with a mean longitudinal velocity  $\bar{v}_z$  of, typically, 20 m/s, and with a full-width-at-half-maximum (FWHM) velocity spread of about 10 m/s. The transverse velocity distribution (FWHM) is about 5 m/s. The decelerated packet leaving the decelerator contains approximately  $10^6$  molecules and has a full spatial extent of about 2 mm along all directions.

While proceeding to the entrance of the microwave resonator in free flight, the decelerated packet spreads out in all directions [Fig. 2(b), I]. If no microwave resonator would be integrated into the setup, the molecules would have to proceed another 128.5 mm of free flight to the detection region, where they are state-selectively detected using a laser-based ionization detection scheme. The laser beam with a waist of about 100  $\mu\text{m}$  is oriented parallel to

the  $x$  axis. In the  $x$  direction, the ion extraction setup limits the detection region to about 2 mm. During this free flight, the packet of molecules spreads out dramatically [Fig. 2(b), II], so that only a small fraction of molecules would still be detected. For the setup with microwave resonator, the molecular cloud is “skimmed” by the entrance and exit holes of the resonator: only the molecules with very low transverse velocities are able to pass [narrow  $v_x$  distribution in Fig. 2(b), III]. However, if the microwave field is turned on with  $P = 3.5$  W coupled into the resonator, the packet of slow ammonia molecules is kept together in transverse directions [Fig. 2(b), III, black circles]. The maximum accepted transverse velocity of our microwave lens for 3.5 W is about  $\pm 3$  m/s in  $x$  direction and about  $\pm 1.6$  m/s in  $y$  direction. The microwave field is turned on as long as the decelerated packet is in the resonator; i.e., 6 ms for molecules with  $\bar{v}_z = 20$  m/s. Note that in the deceleration process of ammonia as applied here, three decelerated packets which are trailing each other by 11 mm are emitted from the Stark decelerator [20]. While flying through the microwave resonator, these three packets will merge.

Figure 3 shows the experimental results for focusing ammonia molecules in their  $|J, K\rangle = |1, 1\rangle$  state. Figure 3(a) displays time-of-flight measurements for  $^{14}\text{NH}_3$  molecules decelerated to  $\bar{v}_z = 20$  m/s for different microwave powers  $P$ , along with Gaussian fits to the observed signal curves. At  $t = 0$ , the decelerated packet leaves the decelerator; i.e., the high voltages at the decelerator are turned off. The signal intensity is increased by about a factor of 8 due to microwave focusing. Furthermore, for increasing power, higher velocities are focused best: compared to the measurements for 2.3 W ( $\epsilon_{\text{MW}} = 1.33$  kV/cm), the maxima of the time-of-flight measurements are shifted to earlier arrival times, and thus higher  $\bar{v}_z$  values, by 0.28 ms for 2.8 W ( $\epsilon_{\text{MW}} = 1.47$  kV/cm) and by 0.43 ms for 3.0 W ( $\epsilon_{\text{MW}} = 1.52$  kV/cm). The highest power of 3.0 W causes overfocusing for the most abundant velocity in the initial velocity distribution, resulting in a reduced signal intensity compared to 2.8 W.

Both the shape of the curves as well as the position of the maxima are reproduced well by Monte Carlo trajectory simulations [see also Fig. 3(b), dashed curves]. However, the intensity increase due to microwave focusing is predicted to be about 1 order of magnitude larger than experimentally observed. This is a strong indication for significant losses in the experiment. One major loss channel might be nonadiabatic transitions [21] to  $M = 0$  states in the low-field regions close to the electric field nodes at the beginning, center, and end of the resonator. One possible way to reduce these losses would be to use the  $TE_{111}$  mode with only one maximum along the longitudinal axis.

The inset of Fig. 3(a) shows the dependence of the observed signal on the microwave power  $P$ . The three measurements shown have been performed for different detection times. For all curves, a steep increase in signal

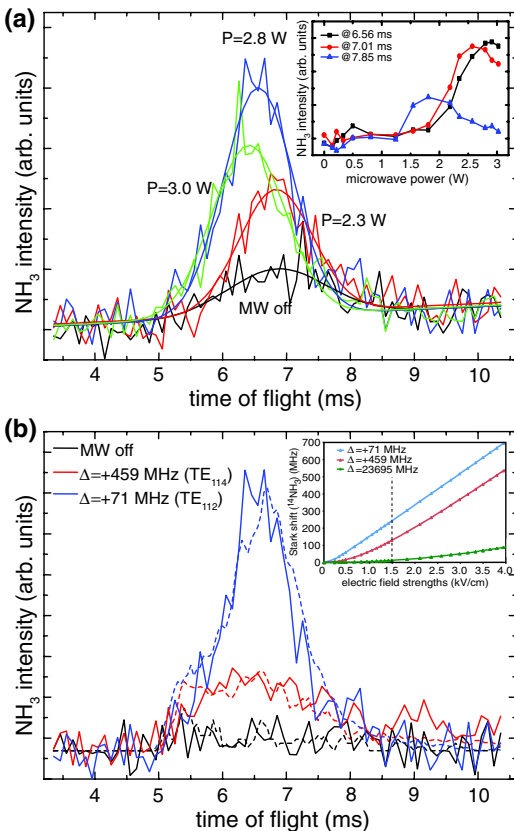


FIG. 3 (color online). Experimental results for focusing ammonia molecules ( $^{14}\text{NH}_3$ ) in their  $|J, K\rangle = |1, 1\rangle$  state decelerated to  $\bar{v}_z = 20$  m/s. (a) Time-of-flight measurements along with Gaussian fits for different microwave powers  $P$  using the  $\text{TE}_{112}$  mode ( $\Delta = +71$  MHz). The inset shows the  $^{14}\text{NH}_3$  intensity as a function of  $P$  for different detection times. (b) Time-of-flight measurements (solid curves) for two different detunings ( $\Delta = +71$  MHz and  $+459$  MHz, respectively) using  $P = 2.8$  and  $0$  W. The dashed curves correspond to Monte Carlo simulations. The inset displays the ac Stark shift (absolute values) for  $^{14}\text{NH}_3$  for two different detunings  $\Delta$  calculated using Eq. (1) along with the corresponding dc Stark shift.

intensity is found with increasing microwave power. For the measurements taken at 7.01 ms, a maximum is obtained at around 2.5 W. For higher microwave power, overfocusing is observed. For a later detection time (7.85 ms) corresponding to slower molecules, the maximum is clearly shifted to lower power (1.8 W), while for an earlier detection time (6.56 ms) and thus faster molecules, it is shifted to higher  $P$  values (around 3 W).

In Fig. 3(b), time-of-flight measurements for  $\bar{v}_z = 20$  m/s slow  $^{14}\text{NH}_3$  molecules using a constant microwave power of 2.8 W ( $\epsilon_{\text{MW}} = 1.47$  kV/cm), but two different detunings are shown. The solid curves are measurements, while the dashed curves correspond to trajectory simulations, which agree well with the experimental results. In the experiment, the signal increase due to focusing amounts to only about a factor of 2 for the  $\text{TE}_{114}$  mode compared to a factor of 8 for the  $\text{TE}_{112}$  mode. This can be explained with a higher probability of nonadiabatic tran-

sitions for the  $\text{TE}_{114}$  mode due to the larger number of low-field regions, and the smaller focusing force for  $\Delta = +459$  MHz compared to  $\Delta = +71$  MHz due to the smaller slope of the Stark shift; 141 MHz/(kV/cm) and 182 MHz/(kV/cm) at 1.5 kV/cm, respectively [inset of Fig. 3(b)]. Note that for the corresponding dc Stark effect the slope of the Stark shift at 1.5 kV/cm is 1 order of magnitude smaller [17 MHz/(kV/cm)].

In summary, we have focused ammonia molecules using a novel microwave lens. The focusing force depends on the particular state, the molecular dipole moment, the sign and magnitude of the detuning of the applied microwave frequency from the molecular resonance frequency, and the microwave field strength. Such a microwave lens can be seen as a first important step towards further manipulation devices, such as a microwave decelerator and trap. Microwave manipulation is a promising route to gain complete control over larger and more complex molecules.

The authors thank J.-U. Grabow, J.M. Doyle, J. Küpper, B. Sartakov, and H. Haak for valuable discussions. H. O. thanks Meiji University for granting him a sabbatical leave at FHI. M. S. acknowledges a Liebig grant from the Fonds der Chemischen Industrie.

\*schnell@fhi-berlin.mpg.de

- [1] E. Wrede, *Z. Phys.* **44**, 261 (1927).
- [2] O. Stern, *Phys. Z.* **23**, 476 (1922).
- [3] J.P. Gordon, H.J. Zeiger, and C.H. Townes, *Phys. Rev.* **95**, 282 (1954); **99**, 1264 (1955).
- [4] S. Y. T. van de Meerakker, H. L. Bethlem, and G. Meijer, *Nature Phys.* **4**, 595 (2008).
- [5] M. Bell and T. Softley, *Mol. Phys.* **107**, 99 (2009).
- [6] M. Schnell and G. Meijer, *Angew. Chem., Int. Ed.* **48**, 6010 (2009).
- [7] P.F. Barker and M.N. Shneider, *Phys. Rev. A* **66**, 065402 (2002).
- [8] R. Fulton *et al.*, *Nature Phys.* **2**, 465 (2006).
- [9] R. Grimm, M. Weidemüller, and Y. Ovchinnikov, *Adv. At. Mol. Opt. Phys.* **42**, 95 (2000).
- [10] R. Hill and T. Gallagher, *Phys. Rev. A* **12**, 451 (1975).
- [11] S. Autler and C. Townes, *Phys. Rev.* **100**, 703 (1955).
- [12] H. L. Bethlem *et al.*, *Phys. Rev. Lett.* **88**, 133003 (2002).
- [13] J. van Veldhoven, H. L. Bethlem, and G. Meijer, *Phys. Rev. Lett.* **94**, 083001 (2005).
- [14] D. DeMille, D. R. Glenn, and J. Petricka, *Eur. Phys. J. D* **31**, 375 (2004).
- [15] K. Enomoto and T. Momose, *Phys. Rev. A* **72**, 061403(R) (2005).
- [16] J.-U. Grabow *et al.*, *Rev. Sci. Instrum.* **76**, 093106 (2005).
- [17] H. L. Bethlem *et al.*, *Phys. Rev. A* **65**, 053416 (2002).
- [18] H. R. L. Lamont, *Methuen's Monographs on Physical Subjects: Wave Guides* (Methuen and Co. Ltd., London, 1950), 3rd ed.
- [19] J. D. Jackson, *Classical Electrodynamics* (John Wiley & Sons, New York, 1998), 3rd ed.
- [20] C. E. Heiner, H. L. Bethlem, and G. Meijer, *Phys. Chem. Chem. Phys.* **8**, 2666 (2006).
- [21] M. Kirste *et al.*, *Phys. Rev. A* **79**, 051401(R) (2009).